Inorg. Chem. **2008**, *47*, 8315−8323

N^2-Functionalized Blue Luminescent Guanosines by 2,2′-Dipyridylamino and 2-(2′-Pyridyl)benzimidazolyl Chelate Groups and Their Interactions with Zn(II) Ions

Sanela Martić, Gang Wu,* and Suning Wang*

Department of Chemistry, Queen's University, Kingston, Ontario K7L 3N6, Canada

Received May 16, 2008

The syntheses of new blue luminescent N^2-modified guanosine derivatives with chromophores *p*-4,4′-biphenyl-NPh_2 (**1a**), *p*-4,4′-biphenyl-N(2-py)$_2$ (**1b**), and *p*-4,4′-biphenyl-2-(2′-pyridyl)benzimidazolyl (**1c**), respectively, have been achieved. These new N^2-guanosines are moderate blue emitters with $\lambda_{max} = 395$ nm (**1a**), 370 nm (**1b**), and 403 nm (**1c**) and $\Phi = 0.13$, 0.07, and 0.10 in tetrahydrofuran, respectively. Spectroscopic studies and density-functional theory calculations established that the guanine moiety and the new chromophore in all three molecules are involved in the luminescent process. We have also established that guanosines **1a**−**1c** can interact with metal ions such as Zn(II). The interactions of Zn(II) ions with the three guanosines were examined via absorption, fluorescence, circular dichroism (CD), and NMR spectroscopic analyses. We have found that these guanosines display a distinct fluorescent response toward Zn(II) ions which can be attributed to the presence of the chelate chromophore N(2-py)$_2$ in **1b** and 2-py-benzimidazolyl in **1c**. For **1a** and **1b**, the addition of Zn(II) ions causes straight fluorescent quenching while for **1c** the addition of Zn(II) ions causes quenching initially, which is followed by a distinct spectral red shift and the intensity enhancement of the new emission peak. NMR and CD studies demonstrated that the Zn(II) ions bind preferentially to the guanine moiety in **1a** and **1b** but to the 2-(2′-py)benzimidazolyl chelate site in **1c**. Moreover, the anion-dependent CD response of **1a**−**1c** toward Zn(II) salts points to the possible involvement of intramolecular hydrogen bonding between the acetate bound to the Zn(II) ion and the hydroxyl groups of the guanosine.

Introduction

Interactions between metal ions and nucleobases are of great importance because along with hydrogen bonding they play important roles in DNA/RNA chemistry and in their applications,[1] including the development of potential metal complexes-based anticancer drugs[2] and DNA-based biosensors for metal ions.[3] As a result, many metal-nucleoside complexes have been investigated and reported previously.[4] Our group has been interested in the development of guanine/guanosine based ligand systems for binding to metal ions because among nucleobases, guanine displays the most versatile hydrogen bonding patterns, including the biologically important G-quartet motif,[5] which may allow us to achieve the assembly of extended systems by taking advantage of both hydrogen bonds and metal−ligand bonds.

* To whom correspondence should be addressed. E-mail: wangs@chem.queensu.ca.

(1) (a) Pyle, A. M. *J. Biol. Inorg. Chem.* **2002**, *7*, 679–690. (b) Li, J.; Zheng, W.; Kwon, A. H.; Lu, Y. *Nucleic Acids Res.* **2000**, *28*, 481–488.

(2) (a) Jiang, P.; Guo, Z. *Coord. Chem. Rev.* **2004**, *248*, 205–229. (b) Breaker, R. R.; Joyce, G. F. *Chem. Biol.* **1995**, *2*, 655–660. (c) Jamieson, E. R.; Lippard, S. J. *Chem. Rev.* **1999**, *99*, 2467–2498. (d) Monchaud, D.; Fichou, M.-P. T. *Org. Biomol. Chem.* **2008**, *6*, 627–636.

(3) (a) Clever, G. H.; Kaul, C.; Carell, T. *Angew. Chem., Int. Ed.* **2007**, *46*, 6226–6236. (b) Lee, A. H. F.; Kool, E. T. *J. Am. Chem. Soc.* **2006**, *128*, 9219–9230.

(4) (a) Purohit, C. S.; Mishra, A. K.; Verma, S. *Inorg. Chem.* **2007**, *46*, 8493–8495. (b) Sigel, H.; Massoud, S. S.; Corfu, N. A. *J. Am. Chem. Soc.* **1994**, *116*, 2958–2971. (c) Anorbe, M. G.; Welzel, T.; Lippert, B. *Inorg. Chem.* **2007**, *46*, 8222–8227. (d) Melchart, M.; Habtemariam, A.; Novakova, O.; Moggach, S. A.; Fabbiani, F. P. A.; Parson, S.; Brabec, V.; Sadler, P. J. *Inorg. Chem.* **2007**, *46*, 8950–8962. (e) Vrabel, M.; Pohl, R.; Klepetarova, B.; Votruba, I.; Hocek, M. *Org. Biomol. Chem.* **2007**, *5*, 2849–2857. (f) Lippert, B. *Coord. Chem. Rev.* **2000**, *200*−*202*, 487–516. (g) Shipman, M. A.; Price, C.; Gibson, A. E.; Elsegood, M. R. J.; Clegg, W.; Houlton, A. *Chem.*−*Eur. J.* **2000**, *6*, 4371–4378. (h) Song, H.; Li, X.; Long, Y.; Schatte, G.; Kraatz, H.-B. *Dalton Trans.* **2006**, 4696–4701.

(5) Davis, J. T. *Angew. Chem., Int. Ed.* **2004**, *43*, 668–698.

10.1021/ic800899b CCC: $40.75
Published on Web 08/19/2008

Chart 1. Structures of **1a**−**1c**

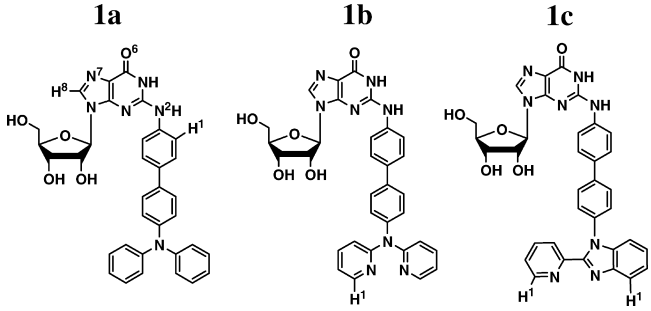

However, the guanine core is perhaps the most difficult to modify by functional groups, among nucleobases, because of the presence of multiple reactive sites. Consequently, examples of guanine/guanosine that are functionalized by a chelate group are still rare.[6] We have been particularly interested in functionalizing guanine/guanosine by fluorescent chromophores since they may allow easy detection/monitoring of the self-assembly of G-quartets and the interactions with metal ions by fluorescence spectroscopy. To maintain the capability of forming G-quartet structures, the hydrogen donor and acceptor sites on the guanine must be preserved, and as a result, the attachment of the fluorescent chromophore to the guanine is limited to the N^2 and C^8 sites. Although examples of C^8- and N^2-functionalized guanosines are known in the literature,[7] to our best knowledge, direct functionalization of guanosines at either the N^2 or the C^8 site by a fluorescent chelate chromophore that can bind to metal ions has not been achieved previously. Hence, little is known on guanosine-based fluorescent sensors/probes for metal ions. Our recent investigation on N^2-functionalized guanosines has shown that the attachment of an aryl group at the N^2 position does not interfere with the hydrogen bonding ability of the base.[8] Therefore, we have chosen to attach a fluorescent 4,4′-biphenyl-based chelate to the N^2 atom of a guanosine. We have synthesized one nonchelating nucleoside N^2-(*p*-4,4′-biphenyl-diphenylamino) guanosine (**1a**) and two chelating nucleosides N^2-(*p*-4,4′-biphenyl-2,2′-dipyridylamino) guanosine (**1b**) and N^2-(*p*-4,4′-biphenyl-2-(2′-pyridyl)benzimidazolyl) guanosine (**1c**). The nonchelate guanosine **1a**is intended for use as a control molecule to elucidate the impact of the chelate groups in **1b** and **1c** on metal ion binding. The structures of the three new molecules are shown in Chart 1.

To demonstrate the potential use of the new guanosines in metal ion binding and metal ion sensing, we have investigated the interactions of the new guanosines with Zn(II) ions, based on the considerations that the Zn(II) ions have many biological functions;[9] the investigation of the interactions of Zn(II) ions with biomolecules such as DNA/RNA and nucleosides is particularly important and challenging because of the lack of convenient spectroscopic handles for sensing Zn(II) ions.[10] The photophysical properties of the new N^2-functionalized guanosines **1a**−**1c** have been investigated. Their interactions with Zn(II) ions in organic solvents have been examined by using absorption, fluorescence, circular dichroism (CD), and NMR spectroscopic methods. The details are presented herein.

Experimental Section

General Information. All reagents were purchased from Aldrich Chemical Co. and used without further purification. Typical coupling reactions were carried under nitrogen atmosphere while the coupling reaction involving guanosine was performed in a sealed tube. All 1D and 2D NMR experiments [correlation spectroscopy (COSY), nuclear Overhauser effect spectrometry (NOESY), and heteronuclear multiple-quantum coherence (HMQC)] were recorded on Bruker Avance 400 or 500 MHz spectrometers at 298 K, unless otherwise specified. CD spectra were recorded on Jasco 715 CD spectrometer in a 1 cm path length cell. The wavelength was varied from 190−600 at 200 nm a minute with 5 overall scans. High-resolution electrospray ionization mass spectrometry (ESI-MS) experiments were performed using the positive ionization mode on QSTAR XL MS/MS Systems using Analyst QS Method. Excitation and emission spectra were recorded on a Photon Technologies International QuantaMaster Model C-60 spectrometer. Quantum yields of compounds **1a**−**1c** were determined using anthracene as the standard in MeOH ($\Phi_{em} = 0.21$), tetrahydrofuran (THF, $\Phi_{em} = 0.30$) and dimethylsulfoxide (DMSO, $\Phi_{em} = 0.22$). The absorbance of all the samples, including the standard, at the excitation wavelength, was approximately 0.097−0.103. The quantum yields were calculated using a previously reported procedure.[11] All UV−vis spectra were collected by using an Ocean Optics Inc. spectrometer and the Spectra Suite software. The Gaussian 03 program suite[12] was used for all molecular-geometry optimization and molecular-orbital calculations. The calculations for the ground state were carried out at the B3LYP level of the theory with 6−311G** as the basis set. Time-dependent density functional theory (TD-DFT) calculations were performed on the optimized ground-state structures.

Synthesis of N^2-(*p*-4,4′-biphenyldiphenylamino) guanosine (1a). To a mixture of *p*-2,2′-diphenylaminiodobiphenyl (**2**) (2.68 g, 5.6 mmol), guanosine (2.38 g, 8.4 mmol), cesium carbonate (2.18 g, 6.7 mmol), and copper(I) iodide (0.16 g, 0.84 mmol, 15%) was added DMSO (8 mL). The solution was degassed with nitrogen for 10 min. A preheated oil bath was used, and the reaction was carried out at 140 °C for 17 h. To the reaction mixture was added water (10 mL), and the solution was neutralized to pH ∼ 7 using

(6) Encinas, S.; Simpson, N. R. M.; Andrews, P.; Ward, M. D.; White, C. M.; Armaroli, N.; Barigelletti, F.; Houlton, A. *New J. Chem.* **2000**, *24*, 987–991.
(7) (a) Sessler, J. L.; Wang, R. *Angew. Chem., Int. Ed.* **1998**, *37*, 1726–1729. (b) Sessler, J. L.; Sathiosatham, M.; Doerr, K.; Lynch, V.; Abboud, K. A. *Angew. Chem., Int. Ed.* **2000**, *39*, 1300–1303. (c) Sessler, J. L.; Jayawickramarajah, J.; Sathiosatham, M.; Sherman, C. L.; Brodbelt, J. S. *Org. Lett.* **2003**, *5*, 2627–2630. (d) Sessler, J. L.; Jayawickramarajah, J. *Chem. Commun.* **2005**, 1939–1949. (e) Kaucher, M. S.; Davis, J. T. *Tetrahedron* **2006**, *47*, 6381–6384. (f) Zhou, L.; Cho, B. P. *Chem. Res. Toxicol.* **1998**, *11*, 35–43. (g) Price, C.; Shipman, M. S.; Rees, N. H.; Elsegood, M. R. J.; Edwards, S. J.; Clegg, W.; Houlton, A. *Chem.—Eur. J.* **2001**, *119*, 4–1201.
(8) (a) Liu, X.; Kwan, I. C. M.; Wu, G.; Wang, S. *Org. Lett.* **2006**, *8*, 3685–3688. (b) Martić, S.; Liu, X.; Wang, S.; Wu, G. *Chem.—Eur. J.* **2007**, *14*, 1196–1204.
(9) Bozym, R. A.; Thompson, R. B.; Stoddard, A. K.; Fierke, C. A. *Chem. Biol.* **2006**, *1*, 103–111.
(10) (a) Kimura, E.; Kikuta, E. *J. Biol. Inorg. Chem.* **2000**, *5*, 139–155. (b) Nolan, E. M.; Jaworski, J.; Okamoto, K.-I.; Hayachi, Y.; Sheng, M.; Lippard, S. J. *J. Am. Chem. Soc.* **2005**, *127*, 16812–16823. (c) Jamieson, E. R.; Lippard, S. J. *Chem. Rev.* **1999**, *99*, 2467–2498.
(11) Murov, S. L.; Carmichael, I. and Hug, G. L. *Handbook of Photochemistry*, 2nd ed.; Marcel Dekker: New York, 1993.
(12) The calculations were performed with the *Gaussian 03* program; Frisch, M.J.; et al. *Gaussian 03*, revision A.9; Gaussian, Inc.: Wallingford, CT, 2004.

aqueous HCl. Further addition of water (30 mL) led to precipitation of the product as a beige solid. The solid was washed further with water to remove unreacted guanosine. The crude solid was further purified using a reverse phase silica gel column with CH_2Cl_2, followed by MeOH/H_2O (4/1) as eluent to give **1a** as a white solid (1.14 g, 35%). Mp >299 °C. ^{1}H NMR (400 MHz, DMSO-d_6) δ 11.8 (broad, s, 1H, N_1H), 10.1 (broad, s, 1H, N_2H), 8.04 (s, 1H, H_8), 7.8 (d, J = 7.4 Hz, 2H), 7.61 (q, J = 2.8, 8.4 Hz, 4H), 7.32 (t, J = 7.7 Hz, 4H), 7.03 (m, 8H), 5.80 (d, J = 5.5 Hz, 1H, $H_{1'}$), 5.47 (d, J = 5.8 Hz, 1H, 2-OH), 5.17 (d, J = 4.3 Hz, 1H, 3-OH), 5.00 (t, J = 5.2 Hz, 1H, 5-OH), 4.55 (d, J = 5.0 Hz, 1H, $H_{2'}$), 4.11 (d, J = 3.6 Hz, 1H, $H_{3'}$), 3.89 (d, J = 3.9 Hz, 1H, $H_{4'}$), 3.63 (m, J = 4.5, 7.3 Hz, 1H, $H_{5'}$), 3.52 (m, J = 4.9, 7.4 Hz, 1H, $H_{5''}$). ^{13}C NMR (400 MHz, DMSO-d_6) δ 151.1, 147.9, 146.8, 139.8, 137.3, 134.9, 133.7, 130.3 (4C), 127.8 (2C), 127.2 (2C), 125.1, 124.7 (4C), 124.5 (2C), 123.8 (2C), 120.1 (2C), 119.2, 115.9, 114.7, 87.8 (C1), 85.9 (C4), 74.4 (C2), 71.1 (C3), 62.2 (C5); ESI-MS m/z 603.1907 $[M + H]^+$. HRMS ESI m/z calcd for $C_{34}H_{30}N_6O_5 \cdot H^+$ $[M + H]^+$ 603.23559, found 603.23565.

Synthesis of N^2-(*p*-4,4′-biphenyl-2,2′-dipyridylamino) guanosine (1b). Compound **1b** was obtained as a colorless solid using the same procedure as described for **1a** by using compound **3** as the starting material (2.98 g, 6.63 mmol) and guanosine (2.21 g, 7.81 mmol) in 29% yield (1.16 g). Mp 226−228 °C. ^{1}H NMR (400 MHz, DMSO-d_6) δ 10.64 (s, 1H, N_1H), 8.96 (s, 1H, N_2H), 8.23 (d, J = 3.85 Hz, 2H), 8.07 (s, 1H, H_8), 7.67 (m, J = 8.27 Hz, 8H), 7.14 (d, J = 8.39 Hz, 2H), 7.03 (m, J = 5.06, 7.16, 8.40 Hz, 4H), 5.78 (d, J = 5.57 Hz, 1H, $H_{1'}$), 5.46 (d, J = 6.04 Hz, 1H, 2-OH), 5.17 (d, J = 4.99 Hz, 1H, 3-OH), 4.98 (m, J = 5.25 Hz, 1H, 5-OH), 4.50 (q, J = 5.47 Hz, 1H, $H_{2'}$), 4.11 (d, J = 4.21 Hz, 1H, $H_{3'}$), 3.89 (d, J = 3.81 Hz, 1H, $H_{4'}$), 3.65 (m, J = 4.18, 4.89, 22.31 Hz, 1H, $H_{5'}$), 3.52 (m, J = 4.67, 6.96, 22.31 Hz, 1H, $H_{5''}$). ^{13}C NMR (400 MHz, DMSO-d_6) δ 158.4, 158.3 (2C), 157.3, 150.6, 150.3, 149.9, 148.9 (2C), 146.3, 147.8, 144.5, 138.7 (2C), 137.2, 134.5, 128.1 (2C), 128.0 (2C), 127.7 (2C), 120.3, 119.2 (2C), 117.6 (2C), 88.1 (C1), 86.1 (C4), 74.6 (C2), 71.0 (C3), 62.1 (C5); ESI-MS m/z $[M + H]^+$ 605.2189, $[M + Na]^+$ 627.3245; HRMS ESI m/z calcd for $C_{32}H_{28}N_8O_5 \cdot H^+$ $[M + H]^+$ 605.2255, found 605.2212.

Synthesis of N^2-(*p*-4,4′-biphenyl-2-(2′-pyridyl)benzymidazolyl) guanosine (1c). Compound **1c** was obtained as a colorless solid using the same procedure as described for **1a** by using compound **4** as the starting material (3.51 g, 7.39 mmol) and guanosine (1.90 g, 6.72 mmol) in 11% yield (0.53 g). Mp 253−256 °C. ^{1}H NMR (500 MHz, DMSO-d_6) δ 10.68 (s, 1H, N_1H), 9.01 (s, 1H, N_2H), 8.39 (d, J = 4.2 Hz, 1H, H^{py}), 8.21 (d, J = 7.88 Hz, 1H, H^{Bn}), 8.09 (s, 1H, H_8), 7.97 (t, J = 7.69 Hz, 1H, H^{Bn}), 7.84 (d, J = 7.46 Hz, 2H), 7.73 (m, 4H), 7.46 (d, J = 8.31 Hz, 2H), 7.37 (m, J = 1.06, 6.53, 7.78 Hz, 5H), 5.81 (d, J = 5.54 Hz, 1H, $H_{1'}$), 5.46 (d, J = 6.05 Hz, 1H, 1-OH), 5.18 (d, J = 4.89 Hz, 1H, 2-OH), 4.99 (d, J = 5.30 Hz, 1H, 3-OH), 4.54 (d, J = 5.41 Hz, 1H, $H_{2'}$), 4.14 (d, J = 4.34 Hz, 1H, $H_{3'}$), 3.93 (d, J = 3.89 Hz, 1H, $H_{4'}$), 3.66 (m, J = 6.88, 11.83 Hz, 1H, $H_{5'}$), 3.64 (m, J = 6.86, 11.83 Hz, 1H, $H_{5''}$); ^{13}C NMR (500 MHz, DMSO-d_6) δ 151.3, 150.7, 149.9, 149.6, 143.2, 139.9, 137.9 (2C), 137.8, 137.7, 128.5, 128.4 (2C), 128.0 (2C), 127.9 (2C), 127.7 (2C), 125.5, 125.1 (2C), 124.8, 123.8, 120.8, 120.4 (2C), 119.4, 111.8, 88.1 (C1), 86.2 (C4), 74.7 (C2), 71.1 (C3), 62.3 (C5); ESI-MS m/z $[M + H]^+$ 629.2216; HRMS ESI m/z calcd for $C_{34}H_{28}N_8O_5 \cdot H^+$ $[M + H]^+$ 629.2260, found 629.2263.

Results and Discussion

Syntheses of Guanosines 1a−1c. To retain the biological activity of guanosines, the hydrogen-bonding sites and the ribose unit must remain intact, which is the key concern in N^2-functionalization. Other considerations that have influenced the design of N^2-functionalized guanosines are fluorescence and the chelating ability of the functional groups. Our earlier investigation has shown that diarylamines such as 2,2′-dipyridylamino and heterocyclic groups such as 2-(2′-pyridyl)benzimidazolyl are highly emissive when attached to an aryl group such as phenyl or biphenyl[13] and are able to chelate to a variety of metal ions, including Zn(II), readily, producing fluorescent or phosphorescent metal complexes.[14] On the basis of these considerations, we decided to incorporate *p*-4,4′-biphenyl-N(2-py)$_2$ and *p*-4,4′-biphenyl-2-(2′-py)benzimidazolyl groups at the N^2-site of guanosine to produce the new guanosines **1b** and **1c**. For comparison purpose, the nonchelating group *p*-4,4′-biphenyl-NPh_2 functionalized guanosine at the N^2 site, **1a**, was also synthesized.

Scheme 1. Synthesis of **1a**−**1c**

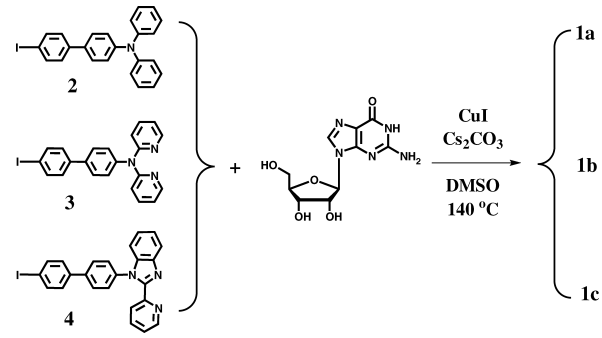

We have found that the Ullmann condensation method, a classic technique that enables the coupling of an aryl halide and an aryl amine in the presence of a base and copper catalyst,[15] is very effective for aryl N^2-functionalization. The synthetic method employed for **1a**−**1c** involves the preparation of appropriate aryl iodide starting materials and their subsequent coupling to guanosine as shown in Scheme 1. The starting materials, aromatic iodides (**2**−**4**), were obtained in moderate yields by the reaction of *p*-diiodobiphenyl with diphenylamine, 2,2′-dipyridylamine, and 2-(2′-pyridyl)benzimidazole, respectively using Ullmann condensation methods reported previously.[16] For the coupling of the aryl iodide with the unprotected guanosine at the N^2 position, controlling the reaction temperature to avoid the nucleoside depurination and the formation of the side products is the key. We have found that the best condition for the synthesis of **1a**−**1c** is to carry out the reaction in DMSO at 140 °C in the presence

(13) (a) Wang, S. *Coord. Chem. Rev.* **2001**, *215*, 79–98. (b) Pang, J.; Marcotte, E. P. J.; Seward, C.; Brown, R. S.; Wang, S. *Angew. Chem., Int. Ed.* **2001**, *40*, 4042–4045. (c) Seward, C.; Pang, J.; Wang, S. *Eur. J. Inorg. Chem.* **2002**, 1390–1399. (d) Kang, Y.; Wang, S. *Tetrahedron Lett.* **2002**, *43*, 3711–3713.

(14) (a) Jia, W. L.; McCormick, T.; Tao, Y.; Lu, J.-P.; Wang, S. *Inorg. Chem.* **2005**, *44*, 5706–5712. (b) Jia, W. L.; Hu, Y. F.; Gao, J.; Wang, S. *Dalton Trans.* **2006**, 1721–1728. (c) Durantaye, L. D. L.; McCormick, T.; Liu, X. Y.; Wang, S. *Dalton Trans.* **2006**, 5675–5682. (d) Kang, Y.; Seward, C.; Song, D.; Wang, S. *Inorg. Chem.* **2003**, *42*, 2789–2797.

(15) (a) Beletskaya, I. P.; Cheprakov, A. V. *Coord. Chem. Rev.* **2004**, *248*, 2337–2364. (b) Liu, Q. D.; Jia, W. L.; Wang, S. *Inorg. Chem.* **2005**, *44*, 1332–1343.

(16) Liu, Q.; Jia, W.; Wu, G.; Wang, S. *Organometallics* **2003**, *22*, 3781–3791.

Table 1. Absorption and Luminescent Spectroscopic Data of **1a**−**1c**[a]

compound	solvent	absorption λ_{max} [nm]	ε_{max} M^{-1} cm^{-1}	λ_{ex} [nm]	λ_{em} [nm]	Q.Y.[b] (Φ_F, %)
1a	THF	238 339	9628 28154	358	395	13
	MeOH	250 295 334	15622 25493 30128	358	406	6.3
	DMSO	261 308 343	13605 22889 29899	320	407	28
1b	THF	220 253 317	24077 17396 37038	346	370 385	7
	MeOH	221 278 313	24277 20686 38268	350	406	0.4
	DMSO	262 278 322	15264 18469 36752	353	387	11
1c	THF	224 258 315	23218 20071 39585	343	403	10
	MeOH	211 258 311	31974 22761 39814	344	401	1.3
	DMSO	265 311	23848 38941	352	423	3.1

[a] All spectra were recorded by using a solution of 6.9×10^{-5} M. [b] Quantum yields were measured relative to anthracene at ambient temperature.

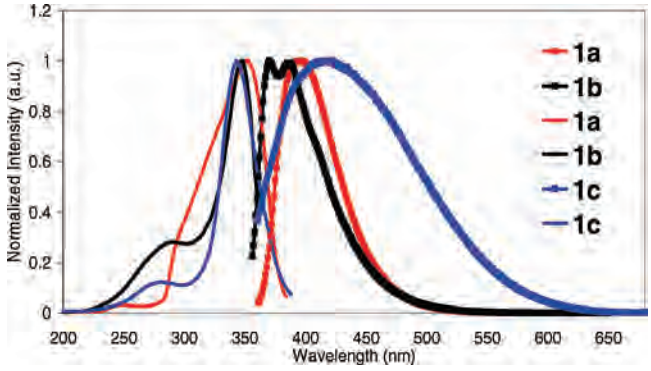

Figure 1. Normalized excitation and emission spectra of compounds **1a**−**1c** in THF (6.9×10^{-5} M).

of CuI and Cs_2CO_3. When this simple procedure was used, the selective arylation at the exocyclic amine without the N^1, N^3 and/or N^7-arylated side products, as determined by NMR, was achieved. Compounds **1a**−**1c** were isolated in moderate yields (11−37%) and were fully characterized using high-resolution mass spectrometry, ^{1}H, ^{13} C, COSY, and HMQC NMR spectroscopy (see Supporting Information).

Photophysical Properties of Guanosines 1a−1c. The absorption and luminescent properties of guanosines **1a**−**1c** are presented in Table 1.**1a**−**1c** display an intense absorption band in the UV region with an absorption maxima at ∼245 nm, typical of the guanine base, and absorption bands in the 270−370 nm region which can be assigned to the π-π* electronic transitions associated with the N^2-aryl substituent. Solvent polarity had little influence on the absorption maxima of the modified guanosines. Compounds **1a**−**1c** emit a bright blue color in solution, when irradiated by UV light, at λ_{em} = 395 nm, 370 nm, and 403 nm, with a quantum efficiency = 0.13, 0.07, and 0.10 in THF, respectively (See Table 1 and Figure 1). Quantum yields of all three compounds are significantly lower in MeOH than in other solvents because of the hydrogen bonding ability of the medium. Because the nonfunctionalized guanosine has no detectable emission bands in the same region, the blue emission of **1a**−**1c** is a direct consequence of the attachment of the biphenyl-diarylamino moiety or the biphenyl-2-(2′-pyridyl)benzimidazolyl group at the N^2 site. In fact, the emission spectral profile of **1a** and **1b** closely resembles that of aryl-NPh_2 and aryl-$N(2\text{-py})_2$, an indication that the emission is most likely from these chromophores. Consistent with this is the fact that the nonfunctionalized N^2-iodophenyl guanosine is only weakly fluorescent with a quantum efficiency of 0.0028. Therefore, the NAr_2 functional group is important in achieving bright luminescent guanosine derivatives. The emission spectrum of **1c** displays a red shift with increasing solvent polarity. In addition, compound **1c** exhibits a very broad emission band that does not resemble that of the corresponding aryl-2-(2′-py)benzimidazole, indicative of the presence of possible multiple emission pathways. Furthermore, **1c** displays excitation-dependent emission (see Supporting Information), further indicating that the emission originates from two different excited states. On the basis of these observations, the emission of **1c** is most likely a combination of electronic transitions that involve the π-π* orbitals and intramolecular charge transfer.

Molecular Orbital Calculations for Guanosines 1a−1c. To understand the electronic and luminescent properties of compounds **1a**−**1c**, we performed molecular orbital calculations. The ground-state structures of all compounds were fully geometry optimized by density-functional theory (DFT) at a B3-LYP/6−311G** level of theory using the Gaussian 03 suite of programs.[12] The optimized structures along with the diagrams of the highest occupied molecular orbital (HOMO) and the lowest unoccupied molecular orbital (LUMO) energy levels for all three compounds are shown in Figure 2, and the computed and experimental HOMO and LUMO energy gaps are given in Table 2. The HOMO and LUMO orbital diagrams for **1a** and **1b** are dominated by π and π* orbitals involving the biphenyl-NAr_2 group and guanine. Hence, the lowest electronic transitions for these compounds may be assigned to π-π* transitions centered on guanine and the biphenyl-NAr_2 group. The MO calculation results indicate that there is little difference between **1a** and **1b** in terms of HOMO and LUMO energies and the nature of their electronic transitions, which is consistent with their similar luminescent properties. In contrast, the HOMO level of **1c** has contributions from the π orbital of the biphenyl and guanine moiety while the LUMO level consists of contributions exclusively from the π* orbitals of the 2-(2′-py)benzimidazolyl group. As a result, the lowest electronic transition in **1c** may be assigned to intramolecular charge transfer from the guanine-biphenyl core to the 2-(2′-pyridyl-)benzimidazolyl group. The DFT calculation results show that there is no conjugation between the 2-(2′-py)benzimidazolyl group and the guanine-biphenyl portion. In fact, these two groups are nearly orthogonal to each other, which is consistent with the previously reported crystallographic data for aryl-2-(2′-py)benzimidazole molecules and is attributable to the nonbonding interaction between the *ortho*-hydrogen

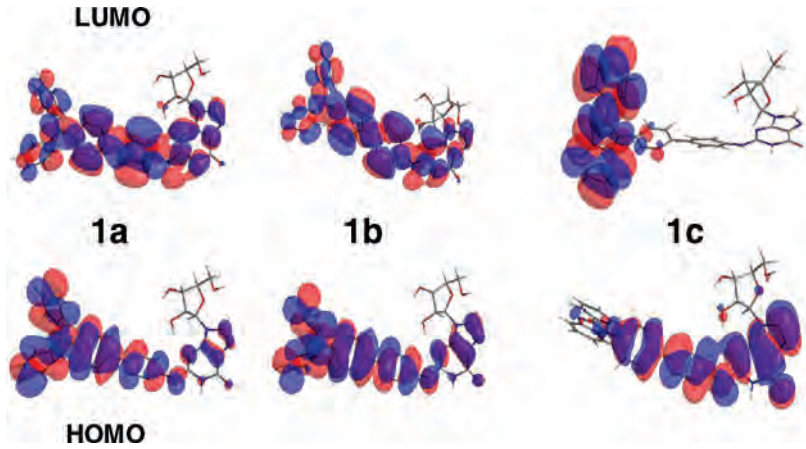

Figure 2. HOMO and LUMO diagrams of **1a**−**1c**.

Table 2. HOMO and LUMO Energy Levels of **1a**−**1c**

	1a	**1b**	**1c**
LUMO (eV)	−1.36	−1.46	−1.65
HOMO (eV)	−5.25	−5.49	−5.87
calculated HOMO−LUMO gap (eV)	3.89	4.02	4.22
optical energy gap (eV) from UV−vis spectra in THF	3.69	3.91	3.92

Table 3. S_0 to S_1 Transition Data of **1a**−**1c** (TD-DFT, B3-LYP/6−311G**)

Compound	Oscillator strength (*f*)	Transition	Energy (nm/eV)
1a	0.81	HOMO→LUMO (67%)	361/3.43
1b	0.88	HOMO→LUMO (67%)	351/3.53
1c	0.60	HOMO→LUMO+1 (64%), HOMO→LUMO (19%)	317/3.91
	0.57	HOMO-1→LUMO (63%)	304/4.08

atoms of the 2-(2-py)benzimidazolyl and the phenyl ring.[13] This lack of conjugation between the chelate chromophore and the guanine-biphenyl unit is clearly responsible for the unique photophysical properties of **1c**.

To further understand the nature of electronic transitions in **1a**−**1c**, we carried out TD-DFT calculations on optimized structures using the Gaussian 03 program. The computed S_0−S_1 electronic transition data for **1a**−**1c** are given in Table 3. For **1a** and**1b**, the transition from the S_0 to the S_1 state involves mainly the HOMO (π) and LUMO (π^*) orbitals, as expected. In contrast, the S_0 to S_1 transition in **1c** is a combination of several transitions, among which the lowest electronic transition involves the HOMO (π of guanine-biphenyl) to LUMO+1 (π^* of guanine-biphenyl) transition (64%) and the HOMO (π of guanine-biphenyl) to LUMO (π^* of 2-(2′-py)benzimidazolyl) transition (19%). The second lowest electronic transition in **1c** is the HOMO-1 (π of 2-(2′-py)benzimidazolyl) to LUMO (π^* of 2-(2′-py)benzimidazolyl) (63%) transition, which is ∼0.2 eV higher in energy than the HOMO−LUMO or HOMO−LUMO+1 transitions. These data support that the S_0 to S_1 transitions in **1c** have mixed contributions from both $\pi \rightarrow \pi^*$ transition centered on either the guanine-biphenyl portion or the 2-(2′-py)benzimidazolyl portion and charge transfer between the guanine-biphenyl moiety and the 2-(2′-py)benzimidazolyl group. This finding is consistent with the broad emission band of **1c** and its solvent dependence.

Interactions of 1a−1c with Zn(II) ions. The interaction of zinc ions with the functionalized guanosines was examined by absorption, fluorescence, CD, and NMR titration experiments in THF. The Zn(II) compounds used in our investigation include $Zn(O_2CCH_3)_2 \cdot 2H_2O$ (**5**), $Zn(O_2CCF_3)_2 \cdot 3H_2O$ (**6**), $Zn(ClO_4)_2 \cdot 6H_2O$ (**7**), $Zn[(S)\text{-}O_2CCH(Br)CH(CH_3)CH_3]_2$ (**8**), and $Zn[(R)\text{-}O_2CCH(Br)CH(CH_3)CH_3]_2$ (**9**). Attempts to isolate zinc(II) complexes with any of the guanosines have not been successful.

Absorption and Fluorescence Study of Zn(II) Binding. The blue emission of compounds **1b** and**1c** stems from the N²-arylamine substituent; hence, any metal ion binding to the 2,2′-dipyridylamino or 2-(2′-py)benzimidazolyl group should have a significant impact on their emission spectra. To establish the role of the guanine site in Zn(II) binding we performed a parallel study using **1a**, a luminescent nonchelating analogue. The absorption and fluorescent spectral change of **1a**−**1c** by titration with Zn(II) salts **5**, **8**, and **9** resembles that of **6**, and thus are not discussed here. The complete data can be found in the Supporting Information. The discussion here focuses on Zn(II) salts **6** and **7**.

Upon addition of either zinc salts **6** or **7**, the emission of **1a** and **1b** is steadily quenched as shown by Figure 3 (the experimental data with **6** are provided in the Supporting Information). For **1b**, in the presence of excess **7**, a weak and broad emission band appears in the 450−550 nm region. Zinc perchlorate is a more effective quencher than zinc trifluoroacetate, as shown by the Stern−Volmer plots in Figure 4, which can be attributed to the fact that the $CF_3CO_2^-$ anion is a much stronger donor than the ClO_4^- anion, and hence can compete more effectively with the guanosines for binding to Zn(II) ions than the ClO_4^- anion can. A similar anion impact on Zn(II) binding has been observed previously.[13,14] Because of the absence of a chelate site in **1a**, the fluorescence quenching observed in **1a** must be the direct result of Zn(II) interactions with the guanine core via most likely the N^7 atom. In fact, binding of a Zn(II) ion surrounded by a tridentate chelate ligand at the N^7-site of guanine has been reported previously.[17]

The change in the absorption spectra of **1a** and **1b** with the addition of **6** are similar (see Supporting Information). In contrast, **7** causes a quite different absorption spectral

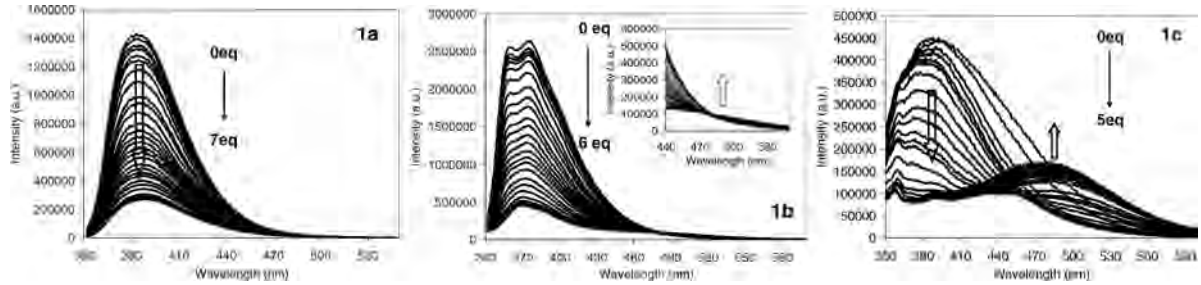

Figure 3. Fluorescence titration spectra of **1a**−**1c** with increasing amount of $Zn(ClO_4)_2$, (**7**) with excitation at 349 nm, 338 nm, and 335 nm, respectively (1.6×10^{-5} M in THF).

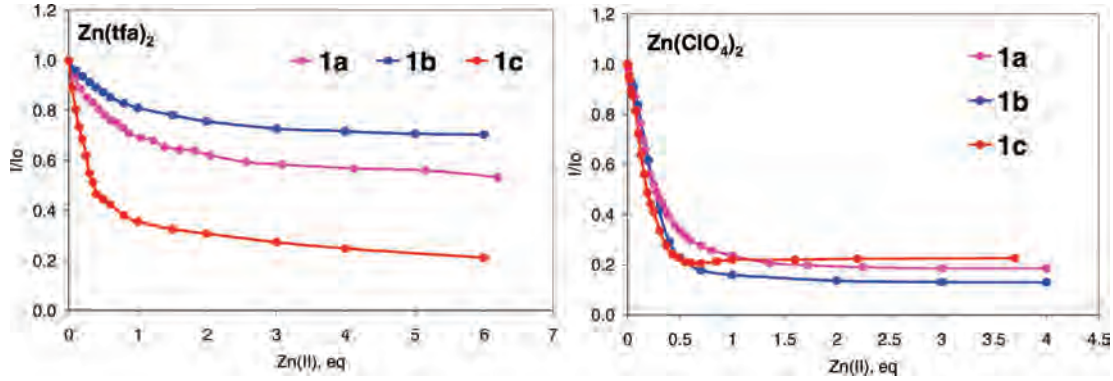

Figure 4. Stern−Volmer plots of **1a**−**1c** titrations by $Zn(tfa)_2$ (**6**) (left) and $Zn(ClO_4)_2$ (**7**) (right) (1.6×10^{-5} M in THF). The emission peak of the free ligands was monitored.

change of **1a** and **1b**: for **1a**, the absorption band at 317 nm experiences some decrease while for **1b**, the same absorption band decreases in intensity and a weak absorption band appears in the 350−450 nm region, an indication that **7** may be interacting with both guanine and the dipyridylamino groups in **1b**, which is consistent with the appearance of a broad weak emission band in the fluorescent titration spectra with **7**. In fact, it has been shown previously that the binding of a Zn(II) ion to a dipyridylamino ligand causes quenching and an emission spectral red shift.[13,14] We also confirmed this by titrating the model compound 4-iodo-biphenyl-N(2-Py)$_2$ (**3**) with **7** that showed the appearance of a broad weak emission band with the addition of Zn(II) ions (see Supporting Information).

The response of **1c** toward Zn(II) ions is unique among the three molecules. As shown in Figure 3, the addition of **7** to **1c** in THF results in quenching of the emission peak at 403 nm but "turning-on" of a new broad emission band at $\lambda_{max} = \sim 490$ nm that increases in intensity with the Zn(II) concentration. The absorption band at $\lambda_{max} = 315$ nm of **1c** also experiences a distinct red shift with the addition of Zn(II) ions. To understand the origin of the emission color change of **1c** with the addition of Zn(II) ions, we carried out the Zn(II) titration experiment with the model compound 4-iodo-biphenyl-2-(2′-py)benzimidazole, **4** (see Supporting Information). The emission spectrum of **4** experiences a significant red shift and a drastic enhancement of intensity upon the addition of **6** and **7**. Our earlier investigation on 2-(2′-py)benzimidazolyl derivative ligands also showed consistently that the binding of a Zn(II) ion to the 2-(2′-py)-benzimidazolyl chelate site causes fluorescence enhancement. On the basis of these observations and the molecular orbital calculation results, the fluorescent response of **1c** toward Zn(II) can be attributed to the binding of the Zn(II) ion to the 2-(2′-py)benzimidazolyl chelate site that quenches the $\pi \rightarrow \pi^*$ emission involving the biphenyl-guanosine and the charge transfer emission between the 2-(2′-py)benzimidazolyl and the biphenyl-guanosine groups but turns on the $\pi \rightarrow \pi^*$ emission of the 2-(2′-py)benzimidazolyl group. The turn-on response of **1c** toward Zn(II) binding is interesting since it makes ratiometric fluorescent sensing of Zn(II) ions possible, a feature that is highly desired in fluorescent sensing technologies because of the elimination of background interference.

As shown by the Stern−Volmer plots in Figures 4, all three compounds have a moderate affinity toward Zn(II) ions. For $Zn(tfa)_2$, compound **1c** clearly shows a much stronger binding than **1a** and **1b**, while for $Zn(ClO_4)_2$, all three compounds appear to have a similar binding strength. The $Zn(tfa)_2$ titration experiments with the model compounds **3** and **4** showed that the binding to the 2-(2′-py)benzimidazolyl group is indeed about 10 times greater than that to the dipyridylamino group (see Supporting Information). The Stern−Volmer plots for the fluorescent titration data of **6** suggest a formation of a 1:1 (ligand versus Zn) complex while that of **7** exhibit initial 2:1 binding stoichiometry for all three compounds. However, we have not been able to fit the data to either a 1:1 or a 2:1 model. It is very likely that at a relatively high concentration of **7**, a complex equilibrium between 2:1, 1:1 (and 1:2 in case of **1b** and **1c** because of the extra chelate site) coexist in solution, making the

(17) (a) Shipman, M. A.; Price, C.; Gibson, A. E.; Elsegood, M. R. J.; Clegg, W.; Houlton, A. *Chem.—Eur. J.* **2000**, *6*, 4371–4378. (b) Li, J.; Zheng, W.; Kwon, A. H.; Lu, Y. *Nucleic Acids Res.* **2000**, *28*, 481–488.

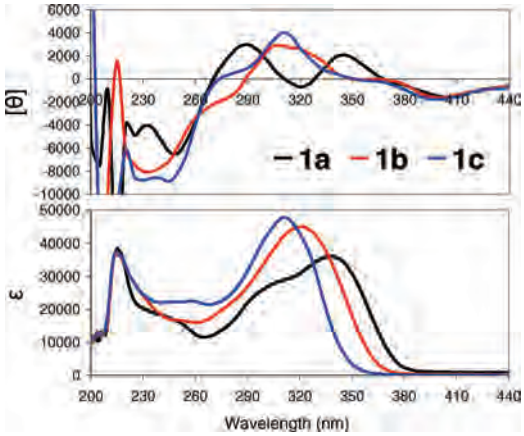

Figure 5. CD (top) and UV−vis (bottom) spectra of **1a**−**1c** (3×10^{-5} M, THF).

extraction of the binding constant challenging. In fact, the 1:1 and 2:1 complexes of **1a** with Zn(II) ions from the solution of **1a** and **7** in DMSO have been positively identified in the ESI-MS spectra (see Supporting Information).

For comparison, we also investigated the fluorescent response of the new guanosines toward $Cd(ClO_4)_2 \cdot 6H_2O$ (**10**) and $Hg(ClO_4)_2 \cdot 3H_2O$ (**11**). Mercury(II) salt **11** causes complete quenching of the emission of **1a** and **1b** and about 90% quenching of the emission of **1c** without the appearance of new emission peaks, which is attributable to the strong heavy atom effects of Hg(II) ion. The response of **10** toward all three compounds is similar to that of **7** except that it is much more sensitive than **7** toward **1b** and **1c** because of the stronger binding of Cd(II) ions toward the dipyridylamino group and the 2-(2-py)benzimidazolyl group (see Supporting Information), a trend that is consistent with previous reports in the literature.[14]

CD Study of Zn (II) Binding. One advantage of using functionalized guanosines as ligands for metal ions is that they are inherently chiral, thus making it possible to examine metal ion binding by CD spectroscopy. In fact, CD has been used frequently as a sensitive tool for the investigation of self-assembly and conformational change of guanosine and its simple derivatives.[18] Monitoring Zn(II) ions binding to nucleotides by CD has also been reported in the literature.[19] As shown by the CD spectra in Figure 5, all three compounds display weak positive bands in the 260−400 nm region in THF that match well with their absorption spectra and are attributable to the luminescent chromophores. In addition, they all have a negative band at ∼250 nm, characteristic of the guanine moiety. The addition of Zn(II) salts to the solutions of **1a**−**1c** causes notable changes to their CD spectra, as shown by the representative CD titration diagram of **1a** with $Zn(OAc)_2$ (**5**) in Figure 6a. Other CD titration diagrams can be found in the Supporting Information. Interestingly, we have found that the degree and the pattern of the induced change are highly dependent on the anion, as shown by the CD spectra of **1a** in the presence of various Zn(II) salts in Figure 6b. Addition of **7** to **1a** causes little change in the 250−400 nm region, while the addition of **6** induces a CD couplet with a positive peak at 320 nm and a negative peak at 355 nm, as well as two negative peaks in the 240−300 nm region. In contrast, **5** induces a CD couplet with a positive peak at 360 nm and two negative peaks in the 250−290 nm region, respectively, that resemble the peaks induced by **6** in the same region. These distinct CD spectral responses by the three different Zn(II) salts indicate that the ribose conformation of the guanosine is likely different with different anions. Because the Lewis basicity of the anions follows the order of $CH_3CO_2^- > CF_3CO_2^- > ClO_4^-$, it is conceivable that the observed CD spectral difference may be influenced by the extent of hydrogen bonding between the anions and ribose. For $CH_3CO_2^-$, internal hydrogen bonds between the oxygen atom of the acetate ligand bound with Zn(II) and the OH group on the $C^{5'}$ of the ribose in **1a** is possible, as supported by molecular modeling (Figure 7), which will certainly provide a greater conformational rigidity to the ribose, thus causing a greater positive enhancement of the 360 nm CD band. For the $CF_3CO_2^-$ anion, a similar internal hydrogen bonding is possible, but because of the reduced Lewis basicity, the H-bond is likely much weaker, thus resulting in less rigid conformation of the ribose, compared to $CH_3CO_2^-$. The ClO_4^- anion is a poor donor and unlikely bound to the Zn(II) ion, and as a result, it is unlikely to form an internal hydrogen bond with the ribose. Other factors such as the coordination geometry and coordination number around the Zn(II) center may also play a role here. The CD response of **1b** toward various Zn(II) salts is similar to that of **1a**, suggesting that the binding environment for a given zinc(II) salt is similar for both guanosines, involving most likely the guanine N^7 site, with possible competitive binding at the 2,2′-dipyridylamino site (Figure 7). The CD response of **1c** toward all Zn(II) salts is weak and no positive enhancement in the 250−400 nm region was observed (see Supporting Information), which is consistent with the binding of Zn(II) ions to the 2-(2′-py)benzimidazolyl site, that is far away from the chiral ribose group, thus producing little impact on the CD spectrum in the region where the chelate chromophore absorbs.

To investigate the binding of guanosines **1a**−**1c** with chiral Zn(II) carboxylates, we examined the CD response of $[Zn[(S)\text{-}O_2CCH(Br)CH(CH_3)CH_3)]_2$ (**8**) or $Zn[(R)\text{-}O_2CCH(Br)CH(CH_3)CH_3)]_2$ (**9**) toward **1a**−**1c** in THF. For **1a** and **1b** the CD spectral change induced by the two chiral zinc carboxylates, in the 250−400 nm region follows the same pattern as that of **5**, with a similar positive CD couplet at 360 nm, indicating that the chirality of the carboxylate bound to the zinc center has little impact on the CD band of the N^2-aryl substituent. However, the positive enhancement at 360 nm by **8** for both **1a** and **1b** is consistently greater than that by **9**, indicative that steric factors do have an impact, although the details have not been fully understood yet. For **1c**, the addition of the chiral Zn(II) salts does not lead to CD couplet formation. The addition of chiral zinc salts to the model compounds **3** and **4** did not yield any significant

(18) (a) Gray, D. M.; Wen, J.-D.; Gray, C. W.; Repges, R.; Repges, C.; Raabe, G.; Fleischhauer, J. *Chirality* **2008**, *20*, 431–440. (b) Gottarelli, G.; Lena, S.; Masiero, S.; Pieraccini, S.; Spada, G. P. *Chirality* **2008**, *20*, 471–485. (c) Shi, S.; Liu, J.; Yao, T.; Geng, X.; Jiang, L.; Yang, Q.; Cheng, L.; Ji, L. *Inorg. Chem.* **2008**, *47*, 2910–2912.

(19) Zimmer, C.; Luck, G.; Holy, A. *Nucleic Acids Res.* **1976**, *3*, 2757–2770.

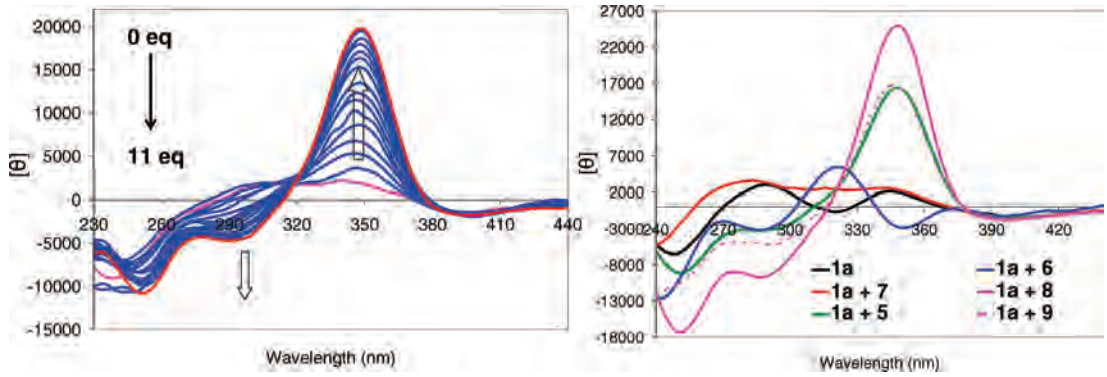

Figure 6. (a) Left: CD titration spectra of **1a** by **5**. b) Right: CD spectra of **1a** in the presence of 5 equiv of various Zn(II) salts (**5**−**9**) (THF, [**1a**]= 3.0×10^{-5} M).

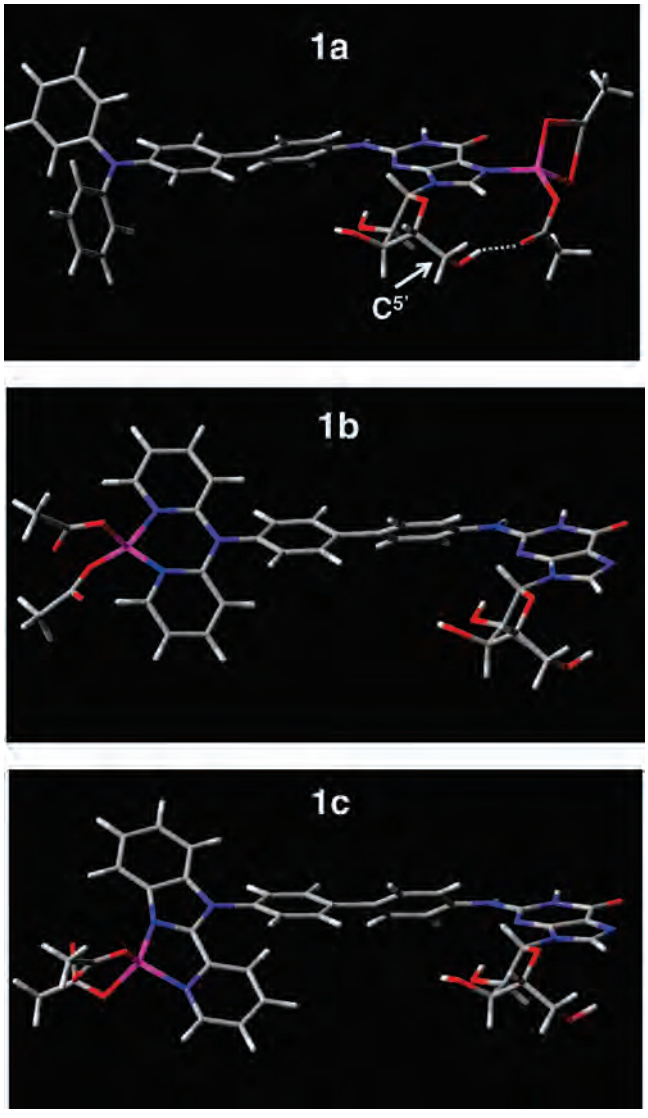

Figure 7. Molecular models showing the binding site of $Zn(OAc)_2$ with **1a**−**1c**. Top: the binding model for **1a** showing intramolecular H-bonding interactions between $C^{5'}$−OH of ribose and one O atom of $Zn(OAc)_2$. This is also one of the binding modes for **1b**. Middle: the 2nd binding mode for **1b** showing the coordination of $Zn(OAc)_2$ at the dipyridylamino site. Bottom: the binding model for **1c** showing the coordination of $Zn(OAc)_2$ at the 2-(2-py)benzimidazolyl site.

CD signals in the 250−400 nm region, as expected. The covalent attachment of the chromophores to the chiral guanosine is clearly important for achieving the distinct CD spectral change of **1a**−**1c** upon binding to Zn(II) ions. The full understanding of the CD spectral response by **1a**−**1c** requires extensive experimental and theoretical work which is beyond the scope of this report.

^{1}H NMR Study of Zn(II) Binding. To determine the binding site of the Zn(II) ions in **1a**−**1c**, ^{1}H NMR titration experiments were performed with Zn(II) salts **6** and **7** in THF-d_8. The partial ^{1}H NMR spectra of titration by **7** are shown in Figure 8, while the NMR titration data by compound **6** can be found in the Supporting Information. Upon the addition of **7** to the solution of **1a**, a well resolved ^{1}H NMR spectrum with a dramatic downfield shift of the H^8 resonance (∼1.0 ppm) was observed, supporting that the Zn(II) ion interacts with the N^7 site of the guanine base. A similar downfield shifting and broadening of the proton peak adjacent to the N^7 binding site in guanine, upon Zn(II) ion coordination, has been reported by Houlton et al.[17] Similarly, the addition of **7** to the solution of **1b** results in a downfield shift of the H^8 resonance by ∼0.1 ppm. Moreover, the pyridyl $H^1{}_{Py}$ resonance at 8.2 ppm in **1b** broadens and experiences a small downfield shift upon the addition of zinc(II), consistent with the binding of zinc(II) ions at both the dipyridylamino site and the guanine N^7 site. The addition of up to 0.2 equiv of **7** to the solution of **1c** (This is the maximum amount that can be added before precipitation occurs because of the poor solubility of **1c**.) results in the immediate broadening of the $H^1{}_{Py}$ peak of the pyridyl ring and the $H^1{}_{Bn}$ peak of the benzimidazolyl group, while the H^8 resonance of the guanine remains unaffected.

The ^{1}H NMR response of **1a**−**1c** to **6** follows the similar pattern as that of **7** in terms of the coordination sites involved. The addition of more than 1 equiv of **6** to **1a** results in the broadening of all signals because of a slow exchange between the bound and free Zn(II) ions, attributable to the relatively strong donor ability of the tfa anion that can compete for binding to Zn(II) with **1a.** The addition of **6** (up to 2.2 eq) to **1b** results in broadening of all pyridyl protons because of the dynamic equilibrium in solution between the bound and free Zn(II) ions, which was confirmed by variable temperature NMR spectra at 190−308 K. At 190 K, a complex pattern with new broad peaks was observed for the spectrum of **1b** with **6**, indicative of the presence of multiple species. Moreover, the broad peaks at δ > 10 ppm attributable to

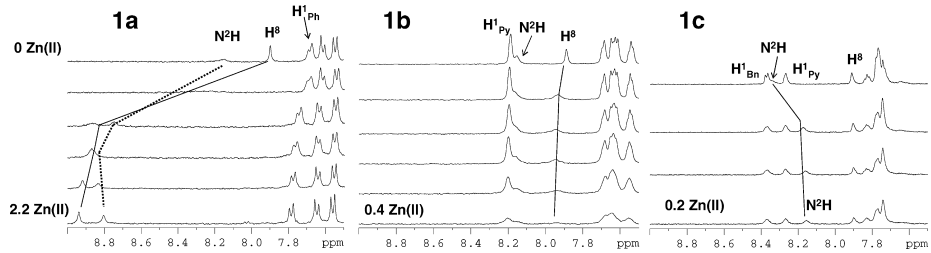

Figure 8. Partial ^{1}H NMR spectra of **1a**−**1c** in the presence of various amounts of $Zn(ClO_4)_2$ ([**1a**] = 1.9×10^{-4} M, [**1b**] = 1.4×10^{-4} M, [**1c**]= 1.5×10^{-4} M, 298 K, THF-d_8).

the imino and amino protons of guanosine involved in hydrogen bonding were also observed, an indication that the complex low temperature NMR spectrum of **1b** in the presence of $Zn(tfa)_2$ likely has contributions from both the Zn(II) complex and oligomeric species formed by hydrogen bonding between guanine units. Similar to **1b**, the ^{1}H NMR spectrum of **1c**-**6** complex is dominated by broad signals over a large temperature range (220−298 K), which can be again attributed to dynamic exchange between the bound and free Zn(II) ions and hydrogen bonding among guanine units at low temperatures. Hydrogen bonds involving the ribose OH groups could not be resolved in ^{1}H NMR spectra because of the poor solubility of the complexes.

Conclusions

On the basis of the fluorescent, CD, and NMR titration data, we can conclude that the preferred binding site for the Zn(II) ions in **1a** and **1b** is the guanine N^7 site. The preference for the N^7 site in a guanine/guanosine by a zinc(II) ion is previously known.[17] For **1b**, the dipyridylamino group, albeit a weaker binding site than the guanosine, is likely competing for the Zn(II) binding. For **1c**, the preferred binding site is the 2-(2′-py)benzimidazolyl chelate because of its high binding affinity for Zn(II) ions. Because of the poor donor capability of the perchlorate anion, $Zn(ClO_4)_2$ may form a 2:1 complex (L/Zn) with the guanosine via either the guanine site or the N^2-functionalized chelate site. In fact, the 2:1 binding mode involving two 2-(2′-py)benzimidazolyl derivative ligands and one Zn(II) ion has been observed previously.[20]

In summary, three new N^2-functionalized luminescent guanosines have been synthesized. We have shown that these luminescent guanosines can bind to metal ions such as Zn(II) ions. The new highly emissive functional groups attached to the guanosine are very useful for probing metal-guanosine interactions via both fluorescent and CD modes. In the fluorescent mode, compound **1c** has a unique turn-on response toward Zn(II) or Cd(II) ions. In the CD mode, both **1a** and **1b** are highly responsive to Zn(II) acetate and the derivatives. While N^2-fluorescent nucleosides are not capable of effective chiral discrimination in CD, they are efficient in distinguishing different anions associated with the zinc(II) ion. Investigations of the interactions between functionalized guanosines **1a**−**1c** and other metal ions and their impact on the self-assembly of guanosines such as G-quartet formation are underway, and the results will be reported in due course.

Acknowledgment. We thank the Natural Sciences and Engineering Research Council of Canada for financial support. We are in debt to Dr. Yimin She for his assistance in ESI-MS experiments and Theresa McCormick for her help in CD experiments.

Supporting Information Available: The complete absorption, fluorescence and CD titration data of **1a**−**1c** with **5**−**11**, 1D and 2D NMR data for **1a**−**1c**, ESI-MS spectra for **1a/7**, and ^{1}H NMR titration data of **1a**−**1c** with **6** and **7**. This material is available free of charge via the Internet at http://pubs.acs.org.

IC800899B

(20) Liu, S.-F.; Wu, Q.; Schmider, H. L.; Aziz, H.; Hu, N.-X.; Popović, Z.; Wang, S. *J. Am. Chem. Soc.* **2000**, *122*, 3671–3678.